Quantum Manipulation of Two-Electron Spin States in Isolated Double Quantum Dots

Benoit Bertrand,[1,2] Hanno Flentje,[1,2] Shintaro Takada,[1,2,3] Michihisa Yamamoto,[3,4] Seigo Tarucha,[3,5] Arne Ludwig,[6] Andreas D. Wieck,[6] Christopher Bäuerle,[1,2] and Tristan Meunier[1,2,*]

[1]*Université Grenoble Alpes, Institut NEEL, F-38042 Grenoble, France*

[2]*CNRS, Institut NEEL, F-38042 Grenoble, France*

[3]*Department of Applied Physics, University of Tokyo, Tokyo 113-8656, Japan*

[4]*PRESTO-JST, Kawaguchi-shi, Saitama 331-0012, Japan*

[5]*RIKEN Center for Emergent Matter Science (CEMS), 2-1 Hirosawa, Wako-Shi, Saitama 31-0198, Japan*

[6]*Lehrstuhl für Angewandte Festkörperphysik, Ruhr-Universität Bochum, Universitätsstrasse 150, 44780 Bochum, Germany*

(Received 2 December 2014; published 28 August 2015)

We studied experimentally the dynamics of the exchange interaction between two antiparallel electron spins in an isolated double quantum dot where coupling to the electron reservoirs can be ignored. We demonstrate that the level of control of such a double dot is higher than in conventional double dots. In particular, it allows us to couple coherently two electron spins in an efficient manner following a scheme initially proposed by Loss and DiVincenzo [Phys. Rev. A 57, 120 (1998)]. The present study demonstrates that isolated quantum dots are a possible route to increase the number of coherently coupled quantum dots.

DOI: 10.1103/PhysRevLett.115.096801 PACS numbers: 73.21.La, 03.65.-w, 03.67.-a, 78.67.Hc

An important stream of research is nowadays to develop tools to operate and control quantum nanocircuits at the single-electron level. The coherent manipulation of the spin of an electron trapped in a quantum dot is now well established [1–3]. Some of the most advanced spin manipulation schemes take advantage of the important control of quantum dot systems defined with lateral gates in a two-dimensional electron gas (2DEG). However, the possibility to exchange electrons between the dot and the reservoir reduces the available tuning parameter space and renders the manipulation of multidots almost intractable. Isolating the dot system from the reservoirs [4,5] could therefore not only restore its full tunability but could also remove parasitic effects occurring during electron spin manipulation such as photon-assisted tunneling [6].

Here we demonstrate that coupled quantum dots can be defined and well controlled in an isolated configuration above the Fermi energy, where the coupling to the electron reservoir can be ignored. The tunnel coupling t between the dots can be easily tuned at nanosecond time scale over several orders of magnitude while keeping the number of electrons in the dots constant. This extra tunability of the dots allows us to switch on and off the exchange interaction J between two electron spins by only changing t and to perform controlled exchange oscillations in a scheme initially proposed by Loss and DiVincenzo [7]. In contrast to previous spin qubit experiments where J is controlled with the detuning ϵ between the dot potentials [8], our strategy permits us to maintain the system at a sweet spot with respect to charge detuning noise, and we demonstrate an increase of the number of coherent oscillations within the coherence time. Such a manipulation scheme is directly compatible with a quantum electronic circuit where single-electron transfer is performed with the help of surface acoustic waves (SAWs) [9]. Moreover, the simplification in terms of dot tunability could have an impact on the scaling of coherently controlled quantum dots.

The quantum dot system is fabricated using a GaAs/AlGaAs heterostructure grown by molecular beam epitaxy with a 2DEG 100 nm below the surface. It is formed by local depletion of the 2DEG by means of metal Schottky gates deposited on the surface of the sample. The inset in Fig. 1(a) shows a scanning electron microscopy (SEM) image of the sample used in the experiment. An electrostatic calculation of the potential experienced by the electrons is presented in Fig. 1(b). The left dot, called the charging dot, is the only one connected to the Fermi sea and permits the charging of the isolated double dot with electrons. The right one, called the channel dot, is realized with the two long gates and lies a few meV above the Fermi energy. The voltage V_R applied on the gate R allows us to tune the interdot tunnel coupling t. The voltage V_L applied on the gate L is used to close the barrier between the charging dot and the reservoir but also to change ϵ. Both gates are connected via low-temperature homemade bias tees to high bandwidth attenuated coaxial lines allowing gigahertz manipulation. The frequency range of the bias-tee low-frequency section (dc, 1 MHz) permits fast loading of the electrons. The charge state of the charging dot can be monitored using an on-chip electrometer [a quantum point contact (QPC) defined with the red gate in the inset in Fig. 1(a)] with a 1 kHz detection bandwidth imposed by the room-temperature electronics. Measurements have been performed in a dilution refrigerator with a base temperature of 60 mK. A 100 mT magnetic field is applied in the plane of the 2DEG to lift the degeneracy between antiparallel and parallel two-electron spin states.

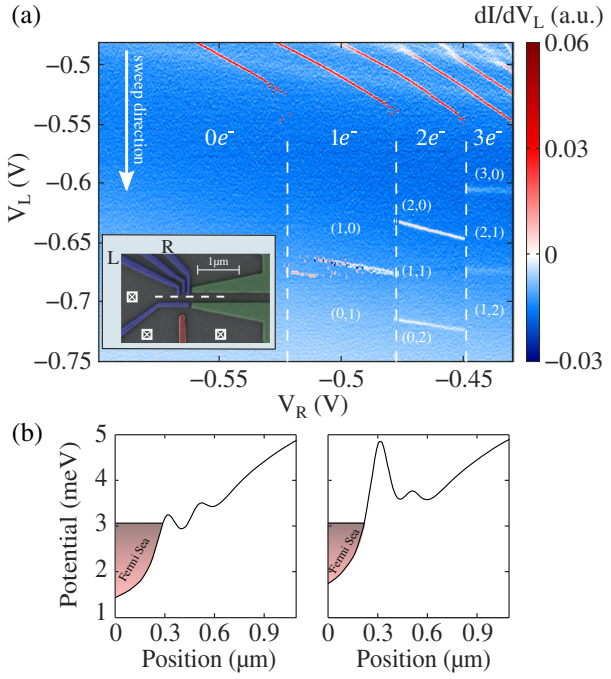

FIG. 1 (color online). (a) Stability diagram of the charging quantum dot. The QPC current is averaged for 3 ms per point; the voltage V_L is swept from more positive to more negative values, whereas V_R is stepped. The signal is then numerically derived with respect to V_L to highlight the changes in the QPC conductance. The number of electrons loaded into the isolated region is changed from 0 to 3 depending on V_R. The label (i, j) refers to i electrons in the charging part and j electrons in the channel part of the isolated double dot. The $(1, 2)/(0, 3)$ transition is hardly visible because of the large interdot tunnel coupling at this position. (Inset) SEM picture of the quantum dot system. (b) Electrostatic calculation of the potential along the white dashed line [(a) inset] for low (left) and high (right) negative V_L. The calculation has been implemented from the gate layout following Ref. [10].

Figure 1(a) shows a charge stability diagram of the charging quantum dot. For $V_L > -0.55$ V, the charging dot is well coupled to its reservoir, and the charge degeneracy lines between $n + 1$ and n electrons are observed down to zero electrons. For $V_L < -0.55$ V, the charge degeneracy lines are disappearing. It indicates that the exchange of electrons between the charging dot and the lead has been suppressed. Therefore, the number of charges trapped in the dot system remains fixed until the end of the sweep and is changed depending on V_R. Deeper in this isolated region [lower part of Fig. 1(a)], additional lines can be seen which are the results of tunneling to the channel quantum dot. Since electron exchange with the leads is suppressed, only the charge distribution between the dots can be varied: for the case of n electrons contained in an isolated double dot, only n charge degeneracy lines are expected. This leads to a drastic simplification of the obtained stability diagrams that could be useful for the control of multidot structures.

In the isolated configuration, we are able to characterize the double dot with a fixed number of electrons over a wide range of gate voltages. It is indeed possible to load first the charging dot with the desired number of electrons and then rapidly promote them into the isolated position with a microsecond gate pulse. Finally, the system is scanned from that position to reconstruct a stability diagram of the isolated double dot. Figure 2 shows the observed stability diagram with the overall electron number fixed to one (two) and exhibits one (two) continuous interdot charge degeneracy lines. Contrary to the case where double dots are coupled to the leads, t can be tuned over many orders of magnitude while keeping the number of electrons constant. Indeed, stochastic tunneling events are observed for the most negative values on V_R [see also the one-electron region in Fig. 1(a) and Ref. [11]], giving a tunnel coupling smaller than the measurement bandwidth (kilohertz). For less negative V_R, the lines are broadened until being too wide to be seen, implying that the tunnel coupling overcomes the effect of temperature (gigahertz). The demonstrated control over t is at the heart of the scheme initially proposed by Loss and DiVincenzo [7] to couple two electron spins efficiently via exchange interaction.

For large t, the exchange coupling J is the dominant interaction, and the singlet is a good eigenstate when one electron is present in each dot. For small t, J becomes negligible with respect to the effective magnetic field

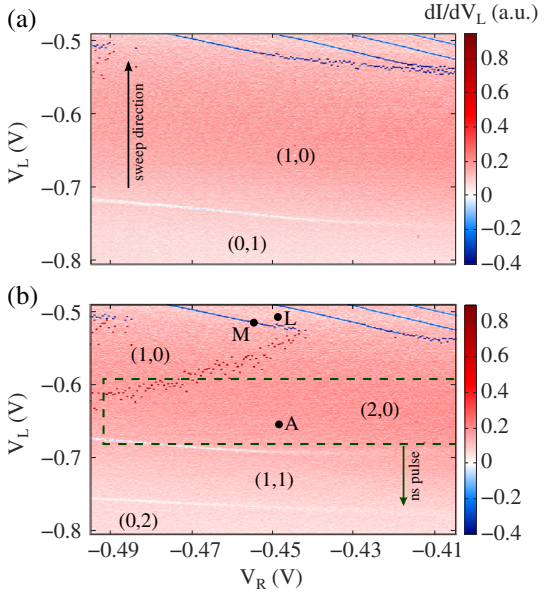

FIG. 2 (color online). Stability diagrams of the isolated double dot with one (a) and two (b) loaded electrons. V_L is swept from negative to positive voltages. The white lines correspond to the charge degeneracy lines of the isolated double dot configuration. The stochastic red events, mostly visible in (b), correspond to tunneling events between the dots and the lead. The points L, M, and A correspond, respectively, to the loading position for two electrons, the two-electron spin measurement position, and a position with two electrons in the isolated charging dot.

gradient Zeeman energy $g\mu_B\Delta B_z$ induced by the hyperfine coupling to the nuclear spins of the heterostructure [12]. As a consequence, mixing between singlet and triplet states occurs. To infer the relative strength between J and $g\mu_B\Delta B_z$, we probe where spin states are mixed in the gate voltage space. The protocol is as follows: two electrons are first loaded in the charging dot [position L in Fig. 2(b)] and initialized in the singlet ground state by waiting longer than the relaxation time; second, the electrons are brought on microsecond time scales to position A; third, we scan the system with a two-pulse procedure: one microsecond pulse that is varied over the dashed green rectangular region depicted in Fig. 2(b) and a fast fixed negative pulse to the gate L of 50 ns duration and of amplitude $V_{\rm ns}$ equal to 80 mV; finally, we proceed to the spin measurement in bringing the system to point M in Fig. 2(b), where energy selective spin read-out is performed [see Fig. 3(a) and Ref. [11]]. The resulting spin-mixing map is presented in Fig. 3(b). In the (2, 0) region, the system remains in the singlet state. Once the (2, 0)-(1, 1) charge transition is crossed, we observe spin mixing in the (1, 1) charge region only for $V_R < -0.40$ V. This is consistent with the small tunneling region identified in Fig. 2, where J is supposed to be smaller than $g\mu_B\Delta B_z$. We confirmed our interpretation by analyzing the typical time scale for mixing. The data are presented in Fig. 3(c) and are characterized by a Gaussian decay of 17 ns, a time scale comparable to the one reported for double dots coupled with the leads [12], corresponding to $g\mu_B\Delta B_z \approx 100$ neV. For $V_R > -0.40$ V, J becomes dominant with respect to $g\mu_B\Delta B_z$ and the system remains in the singlet state. No mixing is observed in this gate voltage region except for a thin line arising from the $S - T_+$ crossing [8]. We can confirm its nature from the line position dependence with the external magnetic field (see [11]). We therefore demonstrate that we can control J with t from $J \ll g\mu_B\Delta B_z$ to $J \gg g\mu_B\Delta B_z$.

To induce coherent flip flops between electron spins, switching J on and off with t has the main advantage of keeping the system in a sweet spot where $dJ/d\epsilon = 0$ [7] [see Fig. 3(b), bottom right panel]. The coherent exchange pulse sequence is presented in Fig. 4(a). A two-electron singlet state is initialized and brought to the isolated double dot in the (2, 0) charge state (point B). A nanosecond pulse on V_L brings the system to the (1, 1) region with large t (point C), where the singlet is still a good eigenstate. The system is then pulsed adiabatically to point D where $J \ll g\mu_B\Delta B_z$ and ends up in the eigenstate of the Overhauser field $|\uparrow\downarrow\rangle$. Finally, a fast V_R pulse of duration τ_E is applied to reach point E with eigenstates back into the $S - T_0$ basis, resulting in a rotation from $|\uparrow\downarrow\rangle$ to $|\downarrow\uparrow\rangle$ at a frequency J/h. A mirror sequence followed by a spin measurement enables us to recover the triplet probability after the rotation.

We start by tuning the system to the sweet spot by choosing the point E at $V_L + V_{\rm ns} = -0.73$ V, which corresponds to the center of the (1, 1) charge region in

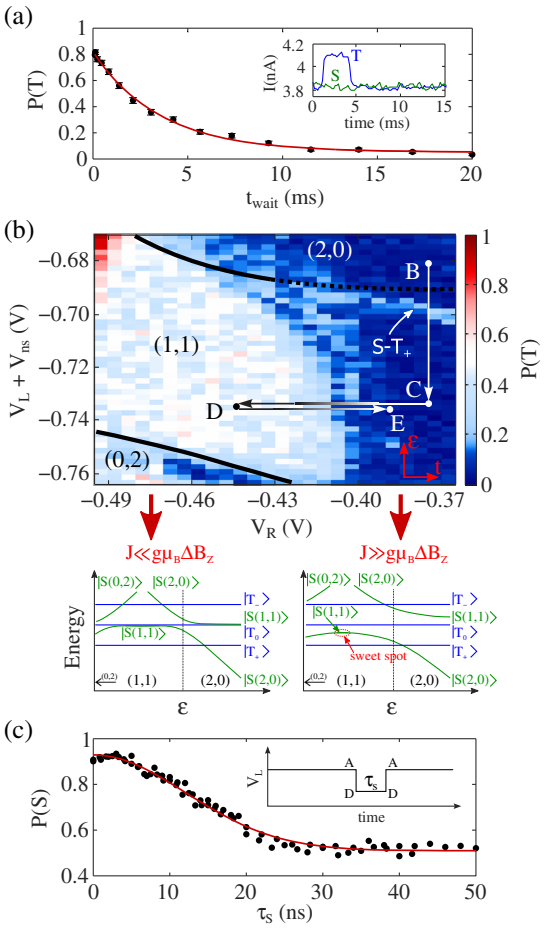

FIG. 3 (color online). (a) Triplet to singlet relaxation. Two electrons are loaded in the left dot at position L [see Fig. 2(b)] mainly in triplet states, and the waiting time is varied to change the triplet proportion. The system is then brought to the isolated position A [see Fig. 2(b)] for 100 μs and finally to position M [see Fig. 2(b)] to perform single-shot energy selective spin read-out [13,14]. This allows us to distinguish single shot the singlet and the triplet states with 80% fidelity. (Inset) Time dependence of the current through the electrometer when a singlet (green lines) or a triplet (blue lines) state is present in the dot. A tunneling event is observed only when the dot is occupied with a triplet state. (b) Spin-mixing map of the two electron spin states (see the text for details). The points B, C, D, and E correspond to positions in the sequence used to perform the coherent exchange oscillations presented in Fig. 4. Each data point is the result of an average over 200 single-shot spin measurements. The corresponding energy diagrams of the two-electron spin states in the isolated double dot for low (left) and strong (right) tunnel coupling are shown below. T_+, T_0, and T_- are the three triplet states in the (1, 1) charge configuration. $S(0,2)$, $S(1,1)$, and $S(2,0)$ are the singlet state, respectively, in the (0, 2), (1, 1), and (2, 0) charge configuration. (c) Measurement of the singlet probability by varying the time spent in the (1, 1) configuration where singlet-triplet mixing occurs. Data are fitted with a Gaussian decay of 17 ns. (Inset) Pulse sequence applied to V_L at $V_R = -0.44$ V.

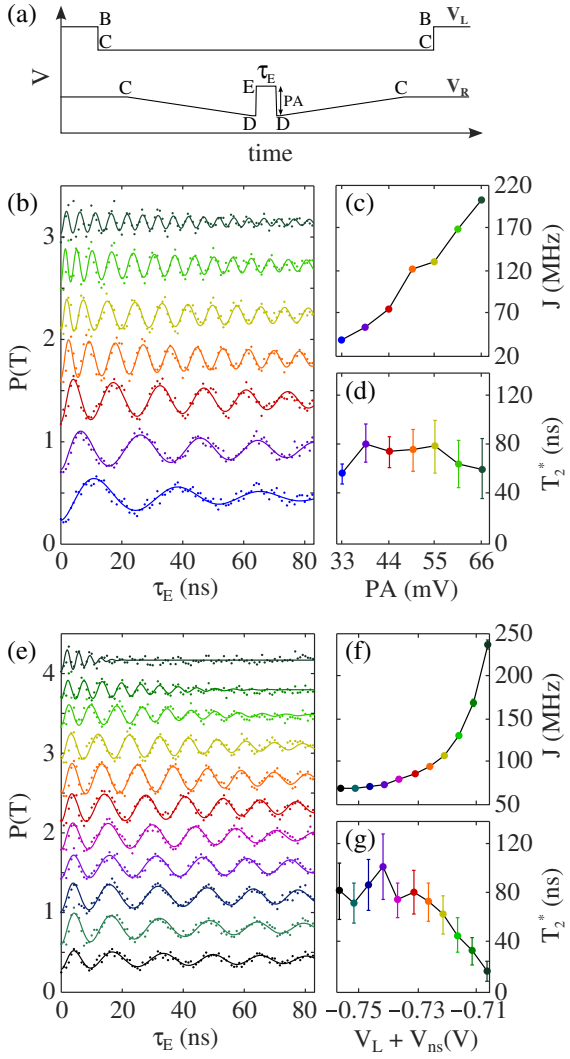

FIG. 4 (color online). (a) Pulse sequence applied on V_L (top trace) and V_R (bottom trace) to induce the coherent exchange oscillations (see the main text for details). (b) Coherent exchange oscillations: triplet probability as a function of τ_E for different PAs with $V_L + V_{ns} = -0.73$ V [see Fig. 3(b)] and (e) for different V_L at fixed PA = 44 mV. Curves are vertically offset for clarity. Solid lines correspond to a fit to the data with a damped oscillatory evolution. Extracted oscillation frequency J as a function of PA (c) and V_L (f). Extracted effective decoherence time T_2^* as a function of PA (d) and V_L (g). The oscillation contrast reaches only 50%, which is attributed to imperfect preparation of the Overhauser field eigenstates via adiabatic passage from the initial singlet state in the charging dot.

Fig. 3(b). The resulting coherent oscillations for different V_R-pulse amplitudes (PAs) are presented in Fig. 4(b). As expected, the larger the PA is, the larger J will be. When fitting the coherent oscillations with a damped oscillatory model, we find an almost linear dependence of J with PA [see Fig. 4(c)]. No significant change in T_2^* is observed [see Fig. 4(d)], which is consistent with the linear dependence of J with PA. This observation is in striking contrast to what is commonly observed when J is controlled with the detuning (see [8,11]).

The system can then be tuned away from the sweet spot by changing the $V_L + V_{ns}$ position of the point E closer to either the (1, 1)-(2, 0) or the (1, 1)-(0, 2) crossings. In our experiment, the coherent oscillations could be performed only for $V_L + V_{ns}$ from -0.76 to -0.71 V, and therefore we focused on the (1, 1)-(2, 0) crossing. In Fig. 4(e), we present a series of coherent exchange oscillations at fixed PAs for different $V_L + V_{ns}$ [see Fig. 3(b)]. We observe a significant acceleration of J as the system approaches the (1, 1)-(2, 0) crossing [see Fig. 4(f)]. It is consistent with the exponential ϵ dependence of J previously reported [8,15]. It implies that the detuning noise sensitivity $dJ/d\epsilon$ also increases exponentially. This is qualitatively consistent with the observed T_2^* reduction [see Fig. 4(g)] and the drastic reduction of the observed number of oscillations. The observed behavior has to be compared with the previous situation where T_2^* remains constant when the oscillation frequency is increased. We therefore demonstrate the improved coherence of the exchange manipulation controlled by the tunneling between the dots.

In conclusion, we have investigated the dynamics of two-electron spin states in an isolated double quantum dot. The full tunability of the dot system allows us to map the mixing process between the two-electron spin states over a wide range of detuning and interdot tunnel coupling. It enabled us to perform coherent spin flip flop between two electron spins by keeping the system in a sweet spot with respect to the detuning charge noise. This work demonstrates coherent manipulations compatible with fast and efficient single-electron transfer with SAWs and paves the way towards the coherent control of multitunnel-coupled quantum dots.

We acknowledge technical support from the technological competence centers of the Institut Néel as well as from Pierre Perrier. M. Y. acknowledges financial support by JSPS, Grant-in-Aid for Scientific Research A (No. 26247050) and Grant-in-Aid for Challenging Exploratory Research (No. 25610070). S. Tarucha acknowledges financial support by JSPS, Grant-in-Aid for Scientific Research S (No. 26220710), MEXT KAKENHHI "Quantum Cybernetics," MEXT project for Developing Innovation Systems, and JST Strategic International Cooperative. A. L. and A. D. W. acknowledge expert help from Dirk Reuter and A. K. Rai and support of the BMBF Q.com-H 16KIS0109, Mercur Pr-2013-0001, and the DFH/UFA CDFA-05-06. T. M. and B. B. acknowledge, respectively, financial support from ERC "QSPINMOTION" and the Fondation Nanoscience.

*Corresponding author.
tristan.meunier@neel.cnrs.fr

[1] R. Hanson, J. R. Petta, S. Tarucha, and L. M. K. Vandersypen, Rev. Mod. Phys. **79**, 1217 (2007).

[2] M. D. Shulman, O. E. Dial, S. P. Harvey, H. Bluhm, V. Umansky, and A. Yacoby, Science **336**, 202 (2012).
[3] M. Veldhorst *et al.*, Nat. Nanotechnol. **9**, 981 (2014).
[4] A. W. Rushforth, C. G. Smith, M. D. Godfrey, H. E. Beere, D. A. Ritchie, and M. Pepper, Phys. Rev. B **69**, 113309 (2004).
[5] A. C. Johnson, C. M. Marcus, M. P. Hanson, and A. C. Gossard, Phys. Rev. B **71**, 115333 (2005).
[6] F. H. L. Koppens, C. Buizert, K. J. Tielrooij, I. T. Vink, K. C. Nowack, T. Meunier, L. P. Kouwenhoven, and L. M. K. Vandersypen, Nature (London) **442**, 766 (2006).
[7] D. Loss and D. P. DiVincenzo, Phys. Rev. A **57**, 120 (1998).
[8] J. R. Petta, A. C. Johnson, J. M. Taylor, E. A. Laird, A. Yacoby, M. D. Lukin, C. M. Marcus, M. P. Hanson, and A. C. Gossard, Science **309**, 2180 (2005).
[9] S. Hermelin, S. Takada, M. Yamamoto, S. Tarucha, A. D. Wieck, L. Saminadayar, C. Bäuerle, and T. Meunier, Nature (London) **477**, 435 (2011).
[10] J. H. Davies, I. A. Larkin, and E. Sukhorukov, J. Appl. Phys. **77**, 4504 (1995).
[11] See Supplemental Material at http://link.aps.org/supplemental/10.1103/PhysRevLett.115.096801 for details.
[12] A. C. Johnson, J. R. Petta, J. M. Taylor, A. Yacoby, M. D. Lukin, C. M. Marcus, M. P. Hanson, and A. C. Gossard, Nature (London) **435**, 925 (2005).
[13] J. M. Elzerman, R. Hanson, L. H. Willems van Beveren, B. Witkamp, L. M. K. Vandersypen, and L. P. Kouwenhoven, Nature (London) **430**, 431 (2004).
[14] T. Meunier, K. J. Tielrooij, I. T. Vink, F. H. L. Koppens, H. P. Tranitz, W. Wegscheider, L. P. Kouwenhoven, and L. M. K. Vandersypen, Phys. Status Solidi (b) **243**, 3855 (2006).
[15] R. Thalineau, S. R. Valentin, A. D. Wieck, C. Bäuerle, and T. Meunier, Phys. Rev. B **90**, 075436 (2014).